Atmos. Meas. Tech. Discuss., 6, 9467–9511, 2013
www.atmos-meas-tech-discuss.net/6/9467/2013/
doi:10.5194/amtd-6-9467-2013

Atmospheric Measurement Techniques Discussions
Open Access

Measuring SO_2 ship emissions with an ultra-violet imaging camera

A. J. Prata

Nicarnica Aviation AS, 2007 Kjeller, Norway

Received: 6 September 2013 – Accepted: 16 October 2013 – Published: 5 November 2013

Correspondence to: A. J. Prata (fp@nicarnicaaviation.com)

Published by Copernicus Publications on behalf of the European Geosciences Union.

Abstract

Over the last few years fast-sampling ultra-violet (UV) imaging cameras have been developed for use in measuring SO_2 emissions from industrial sources (e.g. power plants; typical fluxes ~ 1–$10\,kg\,s^{-1}$) and natural sources (e.g. volcanoes; typical fluxes ~ 10–$100\,kg\,s^{-1}$). Generally, measurements have been made from sources rich in SO_2 with high concentrations and fluxes. In this work, for the first time, a UV camera has been used to measure the much lower concentrations and fluxes of SO_2 (typical fluxes ~ 0.01–$0.1\,kg\,s^{-1}$) in the plumes from moving and stationary ships. Some innovations and trade-offs have been made so that estimates of the fluxes and path concentrations can be retrieved in real-time. Field experiments were conducted at Kongsfjord in Ny Ålesund, Svalbard, where emissions from cruise ships were made, and at the port of Rotterdam, Netherlands, measuring emissions from more than 10 different container and cargo ships. In all cases SO_2 path concentrations could be estimated and fluxes determined by measuring ship plume speeds simultaneously using the camera, or by using surface wind speed data from an independent source. Accuracies were compromised in some cases because of the presence of particulates in some ship emissions and the restriction of single-filter UV imagery, a requirement for fast-sampling (> 10 Hz) from a single camera. Typical accuracies ranged from 10–30 % in path concentration and 10–40 % in flux estimation. Despite the ease of use and ability to determine SO_2 fluxes from the UV camera system, the limitation in accuracy and precision suggest that the system may only be used under rather ideal circumstances and that currently the technology needs further development to serve as a method to monitor ship emissions for regulatory purposes.

AMTD
6, 9467–9511, 2013

1 Introduction

There is strong interest in measuring volcanic gases (e.g. SO_2, HCl, CO_2) in order to provide insights into important processes, for example for monitoring of volcanic gas flux rate changes in reawakening volcanoes in order to forecast future behaviour. Measurements of volcanic SO_2 also helps to constrain the budget of the atmospheric sulphur cycle, e.g. Berresheim and Jaeschke (1983) and Graf et al. (1997). In these examples high precision and accuracy are less important; rather the priority is one of some quantification of the gas concentration and ideally rapid and safe identification. Polluting gases from industrial sources also need to be monitored, especially in the developing world where industrial emission standards may be low and problematic to enforce. Gases also leak from industrial plants and pipelines, and toxic gas releases from industrial accidents or from deliberate acts require identification and monitoring at a safe distance. These applications have driven the development of new imaging cameras that operate in narrow band intervals within the ultra-violet (280–320 nm) part of the electromagnetic spectrum. Most of these developments have occurred in volcanological research e.g. Bluth et al. (2007), Mori and Burton (2006), Oppenheimer et al. (1998) and Kern et al. (2010) but there is potentially much wider application.

Measurements of emissions of polluting gases from ships at sea or at anchor with engines running are of interest because of the harmful effects these emissions have on the local environment. SO_2 is a toxic gas responsible for many deleterious effects on the environment, including acid rain, smog, and damage to vegetation, and in some cases, to human health. SO_2 degrades air quality and can alter the radiation balance through the formation of aerosols that intercept and scatter light. The European Union (EU) has regulated that S in fuel (causing SO_2 ship emissions) should be controlled within closed waterways, harbours and in proximity to environmentally vulnerable areas. The International Maritime Organisation (IMO) caps the global sulphur content of marine fuel at 3.5 % starting from January 2012 – Annex VI to the International Convention for

AMTD
6, 9467–9511, 2013

the Prevention of Pollution from Ships (MARPOL Annex VI). Preference is for S content at 0.1 or 0.5 % for ships in harbours or at berth.

The European Union has sought advice from the scientific community on the techniques and methods for determining SO_2 emissions within harbours in order to assist with regulatory controls regarding the allowed S content in maritime fuel. The Joint Research Centre (JRC) devised a research activity to investigate potential technologies for this problem. Balzani Lööv et al. (2013) describe the overall research program and the measurement campaigns planned to compare the candidate technologies. This paper focuses on the results of one of the measurement campaigns: the SERENAS-R campaign and complements other papers in this Special Issue. Since the paper introduces, for the first time, the use of a novel UV camera imaging system to quantify ship emissions, some background to the development of the system, example prior measurements, and how the measurement protocol has been developed are necessary. The paper is therefore mostly concerned with introducing a new atmospheric measurement technique and follows these logical steps: the background to the ship experiments and some results from a preliminary campaign are presented first. A brief description of the campaigns is provided followed by a methods section that includes a description of the camera system, calibration of the camera, details on the retrieval method and some specifics on how the relevant parameters are estimated. The main results of the SERENAS-R campaign are provided, but since the comparison to the other measurements made during the campaign are presented in the paper by Balzani Lööv et al. (2013), there is no section on validation in this paper. A brief set of conclusions is given with an emphasis on the novelty of the measurement technique and the current limitations.

2 Background to the ship experiments

As with any new measurement technique, it is necessary to start with a theoretical analysis, build an experimental system and then improve the technique based on expe-

AMTD
6, 9467–9511, 2013

rience and experimental results. Theoretical studies can be found in the papers cited in the Introduction, particularly the paper by Kern et al. (2010). An experimental UV camera system has been described by Bluth et al. (2007), among others. For ship plume measurements, two innovations were needed: a faster sampling UV camera and a high quantum efficiency CCD. Details on the camera system can be found in the Methods section, and we begin with a description of the first measurement campaign.

2.1 SUVEX measurement campaign

A scientific research station has been established over the years at Ny Ålesund, Svalbard at the entrance to a fjord, Kongsfjord (78°55′ N, 11°56′ E), fed by a glacier. Activities at the research station include environmental, marine, tropospheric and upper atmospheric experimental research, among others. During the summer season (May–August), sight-seeing cruise ships of various capacity (up to ~ 3400 passengers in one case) visit the fjord in greater numbers, and either dock or lie at anchor, often with engines running. Emissions from these ships disturb the otherwise pristine atmosphere and can affect the quality of baseline atmospheric measurements made routinely at an elevated site in Ny Ålesund. For two weeks in late July and early August 2009, a fast-sampling UV camera was set-up and used to estimate the SO_2 emissions from visiting cruise ships. The measurement campaign – Svalbard Ultra-Violet camera experiment (SUVEX) permitted the first test of the camera system and served to investigate whether the system could detect and quantify relatively low SO_2 ship fluxes of 2–20 $g\,s^{-1}$. Figure 1 shows an example of the imagery obtained from the camera compared to an ordinary visible light camera. The panel on the top shows a conventional visible light image of the cruise ship Costa Magica slowly steaming into the harbour. The bottom panel shows a UV image (~ 320 nm wavelength) of the same scene taken at almost the same time (but not exactly the same perspective) where the change in absorption of light has been highlighted in colour – this corresponds to SO_2 absorption and possibly some light scatter due to particulate matter in the ship's plume. During the campaign a measurement protocol was established, measurements of emissions from

AMTD
6, 9467–9511, 2013

7 ships were made (sometimes multiple times), quantitative retrievals of the SO_2 path amount calculated and the limitations of the system recognised.

Emissions were measured as the ships entered, departed or remained at anchor within the fjord. In all cases emissions were generally low (mean emission rates $\sim 10\,g\,s^{-1}$); likely due to a combination of the low S content of the fuel used but also due to the low engine speeds. On occasion, ships were seen to emit black-coloured smoke (particulates) and in these circumstances the SO_2 retrieval is highly uncertain as no corrections for absorption by smoke particles were made. The types of measurements are illustrated in the 4 panels of Fig. 2 for the cruise ship Costa Magica as it slowly entered Kongsfjord. The plots show SO_2 path amounts (also referred to as path concentrations or concentration multiplied by path length) in units of ppm m[1]. Each panel is separated in time by about 30 s. Retrievals are compromised by contrast changes in the background light due to reflections off the ship, buildings and other objects. Consequently no retrievals were attempted below a limiting height, indicated in the plots by the horizontal line. The emissions from the single funnel on the ship are clearly evident and sequences of images reveal that the retrievals are robust and consistent. The SO_2 emissions appearing ahead of the ship are due to emissions from the Ny Ålesund power plant and qualitative analysis of the imagery show a small plume emanating from the third stack in the row of four (counting from the left). Ships at anchor or manoeuvring slowly within the fjord also emitted SO_2 and some examples are shown in Fig. 3. The lower panels reveal another limitation in obtaining retrievals from a single filter UV camera system as the UV reflected light from the mountains in the background cannot be properly accounted for; the horizontal line shows the limiting height below which retrievals were not made. On these panels and in the panels of Fig. 2, a rough scale is shown for a notional object at a distance of 2 km from the camera. With a single camera it is not possible to resolve distances and it is impossible to discern whether the ship plumes are moving in the direction of the camera or in the opposite direction. This is another limitation that suggests automated quantitative calculation of ship emissions

[1] At S.T.P. 100 ppm m = $0.262\,g\,m^{-2}$.

AMTD
6, 9467–9511, 2013

will be difficult. Finally, in Fig. 4 and Table 2, fluxes determined by tracking features within sequences of images are presented. The fluxes over quite short intervals (minutes) are easily determined by the analysis procedure (see Sect. 3 for details) and in all cases were very low $< 20\,\mathrm{g\,s^{-1}}$. In the case of the SS Vavilov the mean flux is just $8.6 \pm 2.6\,\mathrm{g\,s^{-1}}$.

2.2 SIRENAS-R measurement campaign

The SIRENAS-R campaign was conducted under the auspices of the European Joint Research Centre (JRC) during September 2009 to investigate the utility of certain technologies for estimating the S content in marine fuel. The motivation for this is to provide the relevant authorities with tools that can quickly assess the fuel S content, determined from emission measurements, for compliance with new European Union directives. Currently the permitted S content in fuel used for shipping is 0.5 % by mass with a new limit to be imposed for ships operating within harbours of 0.1 % by mass. Emission measurements by themselves are not sufficient to determine the mass fraction of S in fuel as they depend on engine efficiency factors as well as the power loading of the engines (see Corbett and Fischbeck, 1997 and Corbett and Koehler, 2003). During the campaign, chemical "sniffers" and three different optical methods were tested; these are described by Balzani Lööv et al. (2013) where detailed descriptions of the methods and an inter comparison of results are presented. Here we describe the UV camera system which was used during the campaign and we provide more detailed results of the measurements of ship plume SO_2 path amount (ppm m or $\mathrm{g\,m^{-2}}$) and flux from ships under steam and at dock. A map of the measurement area is shown in Fig. 5.

2.3 SIRENAS-G measurement campaign

Following the SIRENAS-R campaign the UV camera system was tested from a moving vessel at the entrance to Genoa harbour together with an unmanned aerial vehicle (UAV) with a small electrochemical device, again to measure SO_2. This campaign,

AMTD
6, 9467–9511, 2013

SIRENAS-G, was aimed at investigating highly innovative technologies to rapidly monitor ship emissions from moving vessels. Results from this experiment will be reported separately. This paper introduces the technology, explains the experimental procedures and data reduction and describes the main results from the first two experiments.

3 Methods

3.1 UV camera

The UV camera used for these experiments is a highly sensitive CCD array (1344 × 1024 pixels) manufactured by Hamamatsu Photonics, Japan. The quantum efficiency (QE) of the CCD is high from 280–320 nm, which is the main region of interest for measuring SO_2 and some other minor atmospheric polluting gases. The transmission of the lens used and a narrow-band filter are also chosen to have high transmission within the spectral region. Table 1 provides the specifications of the chip and optics, and Fig. shows the filter transmission and QE of the CCD. The main attribute of this camera is that it can sample very quickly (better than 100 Hz) while still maintaing good SNR. This is necessary because the target is often moving (ships under steam) and the signal is quite low – SO_2 emissions are considerably lower than typical volcanic SO_2 emissions (by a factor of 10^4) and lower than industrial stack SO_2 emissions (by a factor of 10^3). The camera is controlled using a laptop with a frame grabber and powered by 12 V batteries or mains power, whichever is more convenient. The system is highly portable, easy to setup and can be ready for operation within 15 min. A photograph of the camera in operation at Hoek van Holland is provided in Fig. 7. The principle of the measurement has been explained in many papers (e.g. Mori et al., 2006; Platt and Stutz, 2008; Tamburello et al., 2011a, b; Kantzas et al., 2010; Dalton et al., 2009; Kern, 2009) and here just a brief description is given.

AMTD
6, 9467–9511, 2013

3.2 Data analysis

SO_2 exhibits significant absorption features within the region between 240–338 nm, due to a series of vibrational bands attributed to the transition $\widetilde{B}^1B_1 - \widetilde{X}^1A_1$ (Kullmer and Demtröder, 1985). The absorption system manifests itself as a series of peaks and troughs at fairly uniform wavelength spacing with decreasing magnitude as wavelength increases. Over the years high resolution spectral absorption measurements have been made for this SO_2 transition, mostly at S.T.P conditions (e.g. Vandaele et al., 1994; Bogumil et al., 2003 and Rufus et al., 2003).

The UV camera measures the backscattered UV light within a narrow band. The focal length of the lens is 50 mm and the total field of view is 7.15° by 5.45°; at a distance of 5 km (line-of-sight, camera to target) the pixel is approximately square with a side length of 0.93 m. Under good lighting conditions, clear sky and small solar zenith angle, a range of 5 km provides acceptable signal to noise.

The data reduction utilises a simple strategy: since there is only a single filter, traditional DOAS: differential optical absorption spectroscopy (see Platt and Stutz, 2008 for details) cannot be used and reliance must be made on good calibration and the geometrical properties of the measurement. Perturbing effects due to light diminution and enhancement along the path, multiple scattering off clouds, water and other objects and scattering and absorption within the band due to other gases (e.g. O_3, NO_2, BrO) and particles must either be ignored (asumed negligible) or modelled in some way. The radiative transfer in realistic situations can be quite complex (see Kern et al., 2010 and Kern, 2009 for an excellent treatment of the problem) and so every effort was made to capture data under optimum conditions, viz. good light, short line-of-sight, low cloudiness, and minimal interference from other gases and particulates. As we shall see it was not always possible to achieve these conditions and some results are certainly degraded because of these effects.

AMTD
6, 9467–9511, 2013

With the assumptions of optimum measurement conditions, the monochromatic radiative transfer problem to be solved may be stated:

$$I(\lambda) = I_0(\lambda)\exp\{-\tau(\lambda, l)\} \tag{1}$$

where I is the measured light intensity at wavelength λ, I_0 is initial intensity before traversing the SO_2 plume and τ is the optical depth,

$$\tau(\lambda, l) = \int_0^L \sigma(\lambda)c(l)\mathrm{d}l, \tag{2}$$

L is the total path traversed by the light. This law is often referred to as the Beer–Bouguer–Lambert law and is strictly valid here for cases with little or no multiple scattering because the extinction coefficient is determined for absorption only. The concentration c along the path l is considered to be constant, reducing Eq. (1) to,

$$\rho = cL = \frac{1}{\sigma_\lambda}\ln\left[\frac{I_0}{I}\right] \tag{3}$$

where ρ is the column mass ($\mathrm{g\,m^{-2}}$) or path concentration, and σ_λ is the photoabsorption cross-section, which is calculated using the laboratory data of Vandaele et al. (1994). With this simplified expression, the retrieval of the SO_2 column consists of making two measurements: one of the light intensity before the light has entered the plume and one of the light intensity after traversing the plume. The absorption coefficient is assumed to be known. In practice the measured radiation is not monochromatic and a further assumption is made that the variations across the narrow band (e.g. due to the absorption coefficient) are small. Kern et al. (2010) has explored various assumptions in the radiative transfer and provides the size of the errors and potential problems when using simplified radiative transfer.

One source of uncertainty lies in the estimation of the background light intensity, I_0. There are several approaches to obtaining I_0, including:

AMTD
6, 9467–9511, 2013

– making measurements away from the plume (e.g. 180° to the plume direction) and assume a uniform background source

– calculating I_0 using a model for the atmosphere based on ancillary atmospheric data

– estimating the background using image measurements and a fitting procedure.

The easiest to implement of these three options is the third and this strategy is described in Sect. 3.4.

3.3 Calibration

Calibration of the camera was conducted in the laboratory using specially designed quartz glass cells with varying thicknesses and a diameter of 50 mm matching the camera lens diameter, and filled with different concentrations of SO_2 gas. Sunlight from a clear sky illuminates the cell and enters the camera through the filter and lens in exactly the same manner as expected in the field. The light intensity behind the cell is estimated using Eq. (1). The cells were filled with differing amounts of SO_2 giving cell path amounts from ~ 100 to ~ 2000 ppm m. The path concentrations were checked using an OceanOptics spectrometer with a fibre optic cable, a blocking filter and utilising a standard UV lamp as a source. As the SO_2 path concentrations from the ship emissions were expected to be low, the camera was set on a high gain setting which provides better sensitivity to low path amounts but also gives noisier imagery. This can be compensated for by using longer exposure times but ultimately there is a trade-off between sensitivity, noise, and exposure times not too long that the ship undergoes noticeable motion. The absorption due to the quartz glass was estimated using an empty cell. For all measurements, a dark signal is removed by capturing images using a blackened plate placed at the entrance to the lens. The calibration

AMTD
6, 9467–9511, 2013

curve is quite linear over the range of path amounts, giving a (linear) least squares fit of:

$$SO_2 = A \ln \left[\frac{DN_0}{DN} \right] + B, \tag{4}$$

where SO_2 is the path amount measured in ppm m, DN_0 are the image digital numbers estimated for the empty cell, and DN are the measured digital numbers for light passing through the cell with SO_2 gas, A and B are the estimated slope and intercept of the linear fit. The resulting fit is shown in Fig. 8. Repeat measurements using the cells with differing solar zenith angles on different days, with variable clear sky atmospheric conditions gave a variability in estimating the logarithm of the ratio of digital numbers (Eq. 4) of ±0.004. The spectrometer measurements provide errors of ~ 3 %. The fit to the absorption measurements using the spectrometer is shown in Fig. 9.

This calibration method permits rapid assessment of the path amounts in ship plumes by simply taking the natural logarithm of the digital numbers. The accuracy is limited principally by the signal-to-noise (SNR) of the measurement and atmospheric conditions. Because the camera offers quite fast sampling, multiple images can be averaged to improve SNR. Digital count differences ($DN_0 - DN$) as low as 5 counts were measured equivalent to ~ 100 ppm m. For a ship plume of ~ 10 m depth, the equivalent SO_2 concentration is ~ 10 ppm or ~ 26 mg m^{-3} at S.T.P. This is considered the lower limit of the measurement capability of the current camera system, under good atmospheric and plume conditions (i.e. bright clear skies and no plume particulates).

Calibration was also performed in the field from time to time using the same cells by inserting them into the camera's field of view while viewing a clear sky. Because the basic principle of the measurement requires a ratio of intensities, changes in gain of the instrument (electronic or optical) are effectively eliminated. The field calibration reduces baseline offsets.

Wavelength response of the camera optics and filter was measured using the OceanOptics spectrometer and the UV lamp in the laboratory. Changes in the filter response function with angle of incidence of UV light and degradation of the filter with

AMTD
6, 9467–9511, 2013

time were not tested, other than through repeat calibrations before and after the field campaign. Since the field of view is quite narrow, unwanted effects due to off-axis light rays are small. No degradation was noticed after 3 months. Alignment of the camera optics was unnecessary as the camera uses a single filter.

3.4 Background intensity, I_0

The strategy for estimating the background intensity makes the assumption that the light intensity in the vicinity of the plume is the same or very similar to that directly behind the plume and assumed to be the main contribution to the light entering the plume and subsequently diminished by absorption and scattering due to SO_2 molecules along the path. Since the field of view angle is quite narrow ($< 8^\circ$) the part of the sky imaged is quite small and so the assumption is reasonable. The optical components that are part of the camera system impart variations across the CCD, even when illuminated by a uniform source. The variation is often referred to as vignetting and is a function of the F/#; it can be reduced by reducing the aperture (increasing the F/#), which is only feasible for bright light conditions with a fast-sampling camera. To illustrate the principle of the method for estimating the background intensity, Fig. 10 shows the image obtained when viewing a calibration cell filled with SO_2 gas only and held up against a bright, clear blue sky. A single transect through the image cutting through the centre of the cell is plotted showing the change in light intensity across the image and across the cell. The drop across the cell is due to SO_2 absorption, while the drop at the edges of the image is due to the vignetting effect. It has been found that the vignetting effect can be modelled very well using a linear combination of a Gaussian and a cubic equation of the form:

AMTD
6, 9467–9511, 2013

$$\mathrm{DN}(p) = A_0 \exp\left(-\frac{x^2}{2}\right) + A_3 + A_4 p + A_5 p^2 + A_6 p^3 \tag{5}$$

$$x(p) = \frac{p - A_1}{A_2},$$

where p is pixel number (measured across the image) and DN is digital number. By using this fitting procedure an estimate of the light intensity behind the attenuated part of the plume can be made. In cases where the ship plume is oriented more in the horizontal than in the vertical, it was necessary to use a vertical transect through the plume. The background intensity was then estimated from a nearby vertical transect that does not intersect the plume. This does, of course, require that some parts of the image are not covered by the plume and that preferably there are clear regions to either side of the plume. It will be seen that for measuring ship plumes this is not a particularly difficult geometry to achieve.

3.5 Emission estimates

Emission estimates require an estimate of the plume speed. One method to do this is to use feature tracking within the plume. UV images of a plume from a power plant stack on the southern side of the shipping channel (see Fig. 5) were used to test the procedure at quite high sampling rates, up to 10 Hz or so. By tracking small features within the plume an estimate of the plume velocity, v_p can be made. If the path concentration is u (gm^{-2}), then by taking a transect (in this case parallel to the y-axis) across the plume and integrating the path concentration, we have

$$w = \int_{y_0}^{y_1} u(y)\mathrm{d}y, \tag{6}$$

AMTD
6, 9467–9511, 2013

where w is now in units of $\mathrm{g\,m^{-1}}$. The y-coordinate must be established from the measuring geometry. For static situations like this the calculation is easily done by knowing the GPS positions of the camera and stack and the elevation of the camera. The field-of-view (FOV) of the camera can be determined from the following:

$$\Psi_i = 2\tan^{-1}\left(\frac{X_i}{2F}\right)$$

where X_i is the chip dimension, i is horizontal or vertical, and F is the focal length of the lens. The physical dimension of a pixel in an image depends on the distance to the object and may be calculated from:

$$Z_i = \frac{2d}{p_i}\tan^{-1}\Psi_i$$

where d is the distance to the object, p_i is the pixel number and Z_i is the pixel size (in m). For the values given above, the angular field-of-view is:

$$\Psi_\mathrm{h} = 7.15°$$
$$\Psi_\mathrm{v} = 5.45°.$$

At a distance of 5 km the pixel is square with side length of 0.93 m.

Given the plume speed, obtained from the data or using ancillary measurements (e.g. local wind speed data), the emission rate, s_e is,

$$s_\mathrm{e} = w v_\mathrm{p}. \tag{7}$$

If the units of plume speed (v_p) are $\mathrm{m\,s^{-1}}$ and the units of w are $\mathrm{g\,m^{-1}}$ then the units of the emission rate are $\mathrm{g\,s^{-1}}$.

It can be seen that an advantage of using fast sampling imagery is that consecutive images can be analysed to determine the movement of the plume, at plume level,

AMTD
6, 9467–9511, 2013

and hence flux or emission rate ($g\,s^{-1}$) can be estimated. This procedure was utilised here but because of the complication that the ships were often moving, not always in a fixed direction, and plume speed can only be estimated in the plane orthogonal to the camera viewing direction, results were best only under certain geometries. Accurate wind speed and direction data were available from a nearby meteorological station established for the measurement campaign at a height of 1.5 m above the surface, so these data could be used in the emission analysis with a height correction (see Sect. 3.7). When possible both methods were utilised.

3.6 Distance calibration

In order to check on the operation of the camera and to ensure the field of view calculations were accurate, measurements of the SO_2 emissions from a nearby stack were made. The location of the stack (see Fig. 5) was approximately due south of site #2 and 1.6 km distant.

3.7 Wind speed

Data from the JRC anemometer located at site #2 were used as input to estimate the wind speed at plume height. A simple relation was used to extrapolate the wind at anemometer height to that at plume height. This is:

$$v(z) = v_0 \left(\frac{z}{z_0}\right)^a, \tag{8}$$

where v_0 is the wind speed at height z_0 and a is an empirically determined constant, taken to be 1/7 (Garratt, 1972). The actual plume speed must be determined from a combination of the wind speed (and direction) at plume height and the ship speed (and direction). The vector component is easy to determine from these speeds and directions, but the ship speed was unknown. Thus for all of the analyses the ship heading was assumed to be 298° for ships leaving the port channel and 118° for ships entering

AMTD
6, 9467–9511, 2013

the port. The ship speed was estimated from the camera imagery by noting the time taken for the ship to pass across the camera. The accuracy of this measurement is very good provided the distance calibration is also good.

4 Errors

Table 3 lists the important sources of error in the retrieval of the concentration path and the emission rate. In this we assume a mean profile retrieval with: path concentration, $u = 100\,\mathrm{ppm\,m}$, mean wind speed, $v_w = 8\,\mathrm{m\,s^{-1}}$, plume width/depth, $L = 10\,\mathrm{m}$, ship speed, $v_s = 4\,\mathrm{m\,s^{-1}}$ for a ship 200 m away. These values give a mean emission rate of $\sim 30\,\mathrm{g\,s^{-1}}$. This analysis suggests that in good visibility conditions, the error is on the order of $\sim 20\,\%$ in the emission rate and $\sim 15\,\%$ in the concentration path. It should be stressed that these errors are probably the least expected as it is assumed that the camera calibration is stable, and more importantly that atmospheric conditions are benign, that is, visibility is good, the sky is bright and uniform (few clouds). It is also assumed that the plume is free of particulates. Visibility can drastically affect the performance of the camera.

5 Results

5.1 SIRENAS-R

Figure 5 shows the locations of the measurements and some important information. Distances to the ships and other targets are needed in order to estimate emission rates, since most of the ships were at sea and moving, and GPS data were not obtained, only approximate values are given. The error in estimating the distances is assumed to be about 10–20 m, which translates to an error in the emission rate of 5–10 %.

The main results are provided in Table 4 and as a series of plots, in the order: (a) a photograph of the ship in the visible, (b) a UV image of the ship and its plume,

AMTD
6, 9467–9511, 2013

and (c) vertical profiles of the camera digital counts and the retrieved profile of the concentration path (in units of ppm m). The main parameters either retrieved or input are provided on the right-hand side panel of the profile plot. Measurements were made over several days, but atmospheric conditions were not always benign and the best data were obtained on 17 and 18 September, 2009. Approximately 50 sets of measurements were made, sometimes on the same ship, including several cases where the ship was at anchor or manoeuvring near a dock. A summary table (Table 4) is included showing all results for 18 September 2009. Note that with only one camera and filter it is not possible to eliminate all types of interference. Hence in many of the plots the profiles are truncated at the lower levels to avoid anomalies due to hard objects (e.g. parts of the ships, land, trees and fixed objects). The main parameters estimated are the SO_2 path amount and the emission rate.

Other results and inter comparisons are provided in Balzani Lööv et al. (2013). Generally, the UV camera overestimates the emissions by as much as 50 % in some cases but on average they agree with independent measurements at the level of 10–20 %. The overestimation is due, in large part, to the presence of particulates in the ship plumes which reduce the UV signal suggesting greater SO_2 and hence larger flux. The speed of the ships has also been neglected and this leads to errors in the estimation of emission rates, that in principle may be of either sign – underestimation or overestimation. This error may be significant because the ships, although moving slowly as they enter the harbour ($< 2\,\mathrm{m\,s^{-1}}$) may still, in the worst case impart an emission rate error directly proportional to $\| v_w - v_s \| / \| v_w \|$. To illustrate the measurement methodology, four case studies are provided.

5.1.1 NYK Cool

NYK Cool operates a fleet of about 30 ships specialising in the transport of perishable items, so-called "reefers" (refrigeration containers). The particular vessel monitored in Rotterdam harbour is registered with IMO 9038323 (*Autumn wind*) and has a length of 158 m, a breadth of 24 m and gross tonnage o 13.077 kt. There is just one main

AMTD
6, 9467–9511, 2013

diesel generator engine of 2000 HP and 700 RPM. The ship was monitored on 18 September 2009 at steam from a distance of approximately 200 m in a wind that was strong enough to cause the ships plume to travel in the direction of the ships motion (Fig. 11). A vertical transect through the plume was used to calculate the SO_2 path concentrations and fluxes. The results are summarised in Table 4 and an example of the vertical profile of SO_2 path concentration is shown in Fig. 12. The emission rates derived are the highest measured, in one case exceeding 170 g s^{-1}. There were no visible signs of particulates in this plume, visibility was good and the distance to the ship was not large so the reason for the high emission rates cannot be easily assigned to measurement conditions. A possible source of overestimation in this case could be due to an overestimate of the apparent wind speed. Since the plume travelled in the direction of ship travel, and the ship speed was not known it is possible that the apparent wind speed has been overestimated. The reported average speed for *Autumn wind* is 11.5 kts (~ 6 m s^{-1}); subtracting this component from the wind speed would result in emission estimates of about half the values given in Table 4 for *NYK Cool*. Even so, the emission rates are still quite high (~ 70–90 g s^{-1}), as are the path concentrations.

5.1.2 NS Concept

The *NS Concept* (IMO 9299692) is a large crude oil tanker with a gross tonnage of 57.248 kt, a length of 244 m and breadth of 42 m. A photograph and UV image of the ship are shown in Fig. 13 and retrieval results shown in Fig. 14. The emission rates determined were in the range 20–30 g s^{-1} which appear to be reasonable for a ship of this size, with an average speed of just under 10 knots.

5.1.3 Stena Hollandica

The *Stena Hollandica* (IMO 9145176) is a super ferry (length 240 m, gross displacement 51.837 kt) that travels from Hoek van Holland to Harwich, UK on a daily basis.

AMTD
6, 9467–9511, 2013

There are four main engines generating 33 600 kW of power. UV images were acquired on several days as the *Stena Hollandica* entered and left the port and also as it manoeuvred at dock. Distance to the ship varied from 500 m to over 2 km and the mean emission was found to be $23.1 \pm 4.1\,\mathrm{g\,s^{-1}}$. The apparent plume speed (combination of the true wind speed and ship speed, measured from the perspective of the UV camera axis) was $\sim 11\,\mathrm{m\,s^{-1}}$. Figure 15 shows visible and UV images of the ferry as it was steaming into the port and and Fig. 16 shows an example vertical profile.

5.1.4 Stena Hollandica – at dock

Data were also captured when the ferry was at dock. In this case the ferry may be considered as approximately stationary, so that any errors in the flux calculation are due to errors in the estimation of the SO_2 path concentration. A sequence of retrievals is shown in Fig. 17. The emissions are larger than independent measurements (by up to a factor of 2) and are likely to be biased high because of particulates in the plume that have not been corrected for. Her sister ferry, *Stena Britannica* (IMO 9419175) with smaller length and less powerful engines gave emission rates from 11–33 $\mathrm{g\,s^{-1}}$, that also appear to be biased high.

The emission rate in the sequence of 8 images has been determined using a constant near surface wind speed of $3\,\mathrm{m\,s^{-1}}$ and a ship speed of $1\,\mathrm{m\,s^{-1}}$. The Stena ferry was manoeuvring near the dock and the engine power was variable which has resulted in a highly variable emission rate of between 20–60 $\mathrm{g\,s^{-1}}$. These are among the highest emission rates measured in the Hoek van Holland channel and it is likely that they are overestimations, due to the particulates in the ship plume. Hobbs et al. (2000) estimated SO_2 emission rates of 3–12 $\mathrm{g\,s^{-1}}$ for 4 sea-going vessels. Isakson et al. (2001) estimate the SO_2 concentration in ship plume in Göteborg harbour, Sweden to be $\sim 4.5\,\mathrm{\mu g\,m^{-3}}$, which corresponds to path amounts of $\sim 0.1\,\mathrm{g\,m^{-2}}$ for path lengths of ~ 100 m, compared to values as high as $0.2\,\mathrm{g\,m^{-2}}$ for path lengths of 10 m measured in this study.

AMTD
6, 9467–9511, 2013

6 Conclusions

Ship plume measurements from an innovative, fast-sampling single-filter UV imaging camera have been made at Kongsfjord, Svalbard and at Rotterdam harbour (Hoek van Holland). A simple scheme was developed to rapidly assess the path amounts (concentration × plume depth in ppm m or g m^{-2}) and emissions can be determined either from the camera imagery itself or by using a surface level wind speed and a model of its variation with height in the first few 100 m of the boundary layer. The camera is able to detect plumes and estimate emissions of SO_2 but with limited accuracy. The purpose of the experiment was to assess the usefulness and reliability of a UV camera system to monitor ship emissions as an aid to estimate the S content of the fuel used. A comparison with other independent measurements of ship plumes during the experiment by Balzani Lööv et al. (2013) show that of four different techniques used, the UV camera gives highest emissions. Currently the system is not able to be used reliably for this purpose as it generally overestimates the emissions, mostly due to the presence of particulates in the plumes (which could not be corrected for). One possible way to alleviate this affect is to make measurements at other wavelengths, as is done in the DOAS technique and correct for the absorption by particles. Thus a camera combined with a spectrometer might be one way to overcome this problem. Another way might be to incorporate more filters with the camera, for example by adding a filter wheel. This approach has the advantage of maintaining full image resolution but will be slower (typically 0.1–1 Hz) and because ships under steam are moving targets, collocation of images at different wavelengths may be problematic. A third more attractive approach is to use two or more cameras with different filters working simultaneously, or preferably a single, dual-path CCD operating at two wavelengths thereby minimising coincidence, maximising sampling frequency and eliminating inter-calibration of CCDs. Improved, realistic radiative transfer can also be implemented. Even after overcoming these mostly technical challenges, there remains the problem of relating the SO_2 emissions to fuel S-content. In order to do that, information on the ships' engines is needed

AMTD
6, 9467–9511, 2013

or a simultaneous measurement of the CO_2 emissions is required. The SO_2 camera may therefore best be suited as a complementary technology used in conjunction with chemical sniffers, active sensing (lidar) and/or a model of ship engine performance.

Acknowledgements. The Joint Research Centre (JRC), Ispra, Italy is thanked for financial support for the SIRENAS-R and SIRENAS-G campaigns. The Norwegian Polar Institute provided funding and logistical support during the SUVEX campaign. Jacob Balzani Lööv, Balint Alföldy and Jens Hjorth (JRC) are thanked for logistical support during the SIRENAS campaigns. NILU scientists Kerstin Stebel, Franck Dauge, and Rolf Haugen provided help and advice in the development of the UV camera system. Are Bäcklund (NILU) assisted at Ny Ålesund during the SUVEX campaign.

References

Balzani Lööv, J., Alföldy, B., Gast, L., Hjorth, J., Lagler, F., Mellqvist, J., Beecken, J., Berg, N., Duyzer, J., Westrate, H., Swart, D., Berkhout, A., Jalkanen, J.-P., Prata, F., van der Hoff, G., and Borowiak, A.: Field test of available methods to measure remotely SO_x and NO_x emissions from ships, Atmos. Meas. Tech. Discuss., in preparation, 2013. 9470

Berresheim, H. and Jaeschke, W.: The contribution of volcanoes to the global atmospheric sulfur budget, J. Geophys. Res.-Oceans, 88, 3732–3740, 1983. 9469

Bluth, G., Shannon, J., Watson, I., Prata, A., and Realmuto, V.: Development of an ultra-violet digital camera for volcanic SO_2 imaging, J. Volcanol. Geoth. Res., 161, 47–56, 2007. 9469, 9471

Bogumil, K., Orphal, J., Homann, T., Voigt, S., Spietz, P., Fleischmann, O., Vogel, A., Hartmann, M., Kromminga, H., Bovensmann, H. Frerick, J., and Burrows, J. P.: Measurements of molecular absorption spectra with the SCIAMACHY pre-flight model: Instrument characterisation and reference data for atmospheric remote-sensing in the 230–2380 nm region, J. Photoch. Photobio. A, 157, 167–184, 2003. 9475

Corbett, J. J. and Fischbeck, P.: Emissions from ships, Science, 278, 823–824, 1997. 9473

Corbett, J. J. and Koehler, H. W.: Updated emissions from ocean shipping, J. Geophys. Res., 108, 4650, doi:10.1029/2003JD003751, 2003. 9473

Dalton, M. P., Watson, I. M., Nadeau, P. A., Werner, C., Morrow, W., and Shannon, J. M.: Assessment of the UV camera sulfur dioxide retrieval for point source plumes, J. Volcanol. Geoth. Res., 188, 358–366, 2009. 9474

Garratt, J.: The Atmospheric Boundary Layer, Cambridge Univ. Press., 1972. 9482

Graf, H.-F., Feichter, J., and Langmann, B.: Volcanic sulfur emissions: estimates of source strength and its contribution to the global sulfate distribution, J. Geophys. Res.-Atmos., 102, 10727–10738, 1997. 9469

Hobbs, P. V., Garrett, T. J., Ferek, R. J., Strader, S. R., Hegg, D. A., Frick, G. M., Hoppel, W. A., Gasparovic, R. F., Russell, L. M., Johnson, D. W., O'Dowd, C., Durkee, P. A., Nielsen, K. E. and Innis, G.: Emissions from ships with respect to their effects on clouds, J. Atmos. Sci., 57, 2570–2590, 2000. 9486

Isakson, J., Persson, T., and Selin Lindgren, E.: Identification and assessment of ship emissions and their effects in the harbour of Göteborg, Sweden, Atmos. Environ., 35, 3659–3666, 2001. 9486

Kantzas, E. P., McGonigle, A., Tamburello, G., Aiuppa, A., and Bryant, R. G.: Protocols for UV camera volcanic SO_2 measurements, J. Volcanol. Geoth. Res., 194, 55–60, 2010. 9474

Kern, C.: Spectroscopic Measurements of Volcanic Gas Emissions in the Ultra-Violet Wavelength Region, Ph.D. Thesis, University of Heidelberg, Heidelberg, Germany, 2009. 9474, 9475

Kern, C., Deutschmann, T., Vogel, L., Wöhrbach, M., Wagner, T., and Platt, U.: Radiative transfer corrections for accurate spectroscopic measurements of volcanic gas emissions, B. Volcanol., 72, 233–247, 2010. 9469, 9471, 9475, 9476

Kullmer, R. and Demtröder, W.: Vibronic coupling in SO_2, and its influence on the rotational structure of the bands in the 300–330 nm region, Chem. Phys., 92, 423–433, 1985. 9475

Mori, T. and Burton, M.: The SO_2 camera: a simple, fast and cheap method for ground-based imaging of SO_2 in volcanic plumes, Geophys. Res. Lett., 33, L24804, doi:10.1029/2006GL027916, 2006. 9469

Mori, T., Mori, T., Kazahaya, K., Ohwada, M., Hirabayashi, J., and Yoshikawa, S.: Effect of UV scattering on SO_2 emission rate measurements, Geophys. Res. Lett., 33, L17315, doi:10.1029/2006GL026285, 2006. 9474

Oppenheimer, C., Francis, P., Burton, M., Maciejewski, A., and Boardman, L.: Remote measurement of volcanic gases by Fourier transform infrared spectroscopy, Appl. Phys. B-Lasers O., 67, 505–515, 1998. 9469

AMTD
6, 9467–9511, 2013

Platt, U. and Stutz, J.: Differential Absorption Spectroscopy, Springer-Verlag, Berlin, Germany, 2008. 9474, 9475

Rufus, J., Stark, G., Smith, P. L., Pickering, J., and Thorne, A.: High-resolution photoabsorption cross section measurements of SO_2, 2, 220 to 325 nm at 295 K, J. Geophys. Res., 108, 5011, doi:10.1029/2002JE001931, 2003. 9475

Tamburello, G., Kantzas, E., McGonigle, A., Aiuppa, A., and Giudice, G.: UV camera measurements of fumarole field degassing (La Fossa crater, Vulcano Island), J. Volcanol. Geoth. Res., 199, 47–52, 2011a. 9474

Tamburello, G., Kantzas, E. P., McGonigle, A. J., and Aiuppa, A.: Vulcamera: a program for measuring volcanic SO_2 using UV cameras, Ann. Geophys.-Italy, 54, 2, DOI: 10.4401/ag-5181, 2011b. 9474

Vandaele, A., Simon, P. C., Guilmot, J. M., Carleer, M., and Colin, R.: SO_2 absorption cross section measurement in the UV using a Fourier transform spectrometer, J. Geophys. Res.-Atmos., 99, 25599–25605, 1994. 9475, 9476

AMTD
6, 9467–9511, 2013

Table 1. Specifications of the Hamamatsu charge-coupled detector (CCD) chip and optics.

Wavelength range	200–600 nm
Pixels	1344 × 1024
Chip size	4.65 µm
UV lens	50 mm f/3.5
UV filter	307 ± 5 nm
Quantum efficiency	30 % 300 nm
Digitisation	12 bits

AMTD
6, 9467–9511, 2013

Table 2. SO_2 emission rates (fluxes) ($g\,s^{-1}$) from 7 ships measured within Kongsfjord, Ny Ålesund either steaming or at anchor. Passenger numbers are indicative only, it is not known whether the ships were at their carrying capacity. No information on the engines or their settings was available at the time of the measurements.

Ship	Gross displacement (tons)	Number of passengers	Emission range ($g\,s^{-1}$)	Activity
Expedition	6336	120	~ 11–14	Manoevering
Mona Lisa	26 678	450	~ 2–4	At anchor
Vavilov	6450	110	~ 6–11	Manoevering
Polar Star	4998	100	~ 4–8	At anchor
Costa Magica	102 587	3470	~ 10–18	Steaming
Columbus	15 000	423	~ 10–15	Steaming
Nordstjernen	2181	100	~ 3-10	Manoevering
Prof. Multanovsky	2140	52	~ 2-8	At anchor

AMTD
6, 9467–9511, 2013

Table 3. Main sources of error in the retrieval of SO_2 path concentration and emission rate from the UV camera. Note that the errors due to visibility have not been included in the final error budget. In practice this error is difficult to characterise and so only data where the visibility is good have been used. Averaging of 10–20 frames is performed in the data analysis and this has the tendency to reduce errors due to noise and atmospheric variability.

Parameter	Uncertainty $1-\sigma$	Impact on retrieval u (ppm m)	Emission rate error, σ_e ($g\,s^{-1}$)
Calibration	±4 counts	±10	±3
Reference profile	±4 counts	±10	±3
Distance	±10 m	±5	±1.5
Ship speed	±0.2 ms^{-1}	–	±1.5
Wind speed	±1 ms^{-1}	–	±2.5
Visibility	**–10–20 counts**	**–25 to–50**	**–7 to–15**
Total rms error		±15	±5

AMTD
6, 9467–9511, 2013

Table 4. SO_2 path amounts and emission estimates from the UV camera for measurements on 18 September 2009.

Time (LT)	Ship name	IMO	Plume height (m)	Plume width (m)	Path concentration ($g\,m^{-2}$)	Error ($g\,m^{-2}$)	Emission rate ($g\,s^{-1}$)	Error ($g\,s^{-1}$)	Apparent plume speed ($m\,s^{-1}$)	Distance
08:38	*Stena Hollandica*	9145176	18.5	10.0	0.195	±0.027	23.1	±4.1	11.7	1200
08:57	*Aura*	9279716	8.0	3.0	0.617	±0.080	17.1	±3.4	9.6	120
11:05	*BCL Iwona*	7000001	14.5	2.5	0.583	±0.079	13.7	±2.5	9.4	200
11:19	*NS Concept*	9299707	18.0	8.0	0.369	±0.051	28.6	±4.9	9.6	600
15:35	*NYK Cool*	9038323	22.0	10.0	1.570	±0.196	174.3	±34.9	11.0	400
15:35	*NYK Cool*	9038323	20.0	9.0	1.491	±0.195	148.3	±29.7	10.9	400
15:35	*NYK Cool*	9038323	19.5	8.0	1.535	±0.195	133.0	±27.9	10.8	400
15:47	*OPDR Tanger*	9389306	20.0	7.0	0.098	±0.015	4.8	±1.0	7.3	600
16:14	*Stena Britannica*	9235517	18.0	4.0	0.786	±0.110	29.6	±5.0	9.5	240
16:14	*Stena Britannica*	9235517	17.0	2.0	0.673	±0.098	11.1	±1.8	9.5	240
16:14	*Stena Britannica*	9235517	16.0	3.0	1.152	±0.147	33.6	±5.4	9.5	240
16:14	*Stena Britannica*	9235517	17.0	1.8	0.771	±0.100	12.7	±2.3	9.5	240
16:56	*Spaarnedijk*	9285457	16.0	2.7	0.445	±0.055	10.2	±2.0	8.3	300
17:01	*Endeavour*	9312595	18.0	6.5	0.518	±0.068	32.6	±6.0	9.6	200
17:27	*STX Ace II*	9443853	17.5	6.1	0.454	±0.064	23.3	±4.7	8.3	760
17:37	*Geest Trader*	9110535	10.0	2.8	0.418	±0.059	7.5	±1.2	6.6	140

AMTD
6, 9467–9511, 2013

Fig. 1. Visible (top panel) and UV (bottom panel) images of the cruise liner *Costa Magica* as it enters Kongsfjord. The plume from the funnel is barely noticeable in visible light, while the UV camera detects a ship plume some distance downwind through a change in the absorption of UV light by SO_2 in the plume.

AMTD
6, 9467–9511, 2013

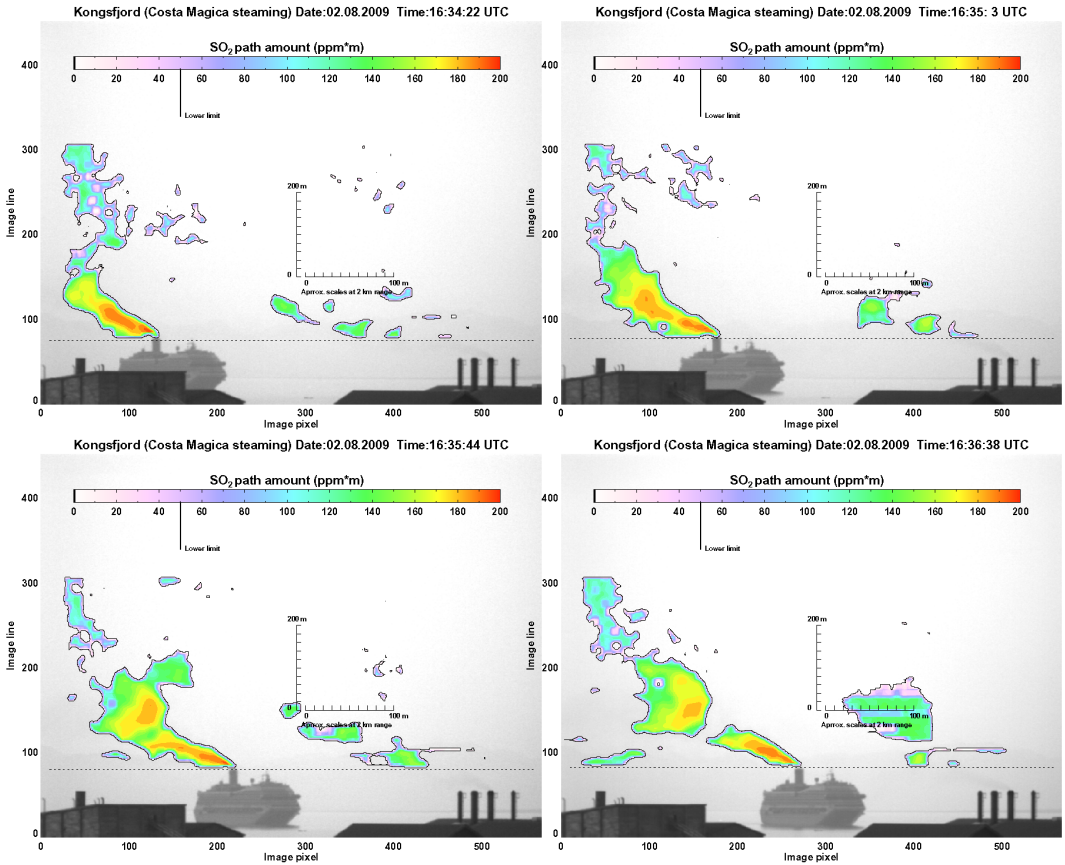

Fig. 2. SO_2 path amounts retrieved from the UV camera for a cruise ship steaming into Konsfjord, Ny Ålesund.

AMTD
6, 9467–9511, 2013

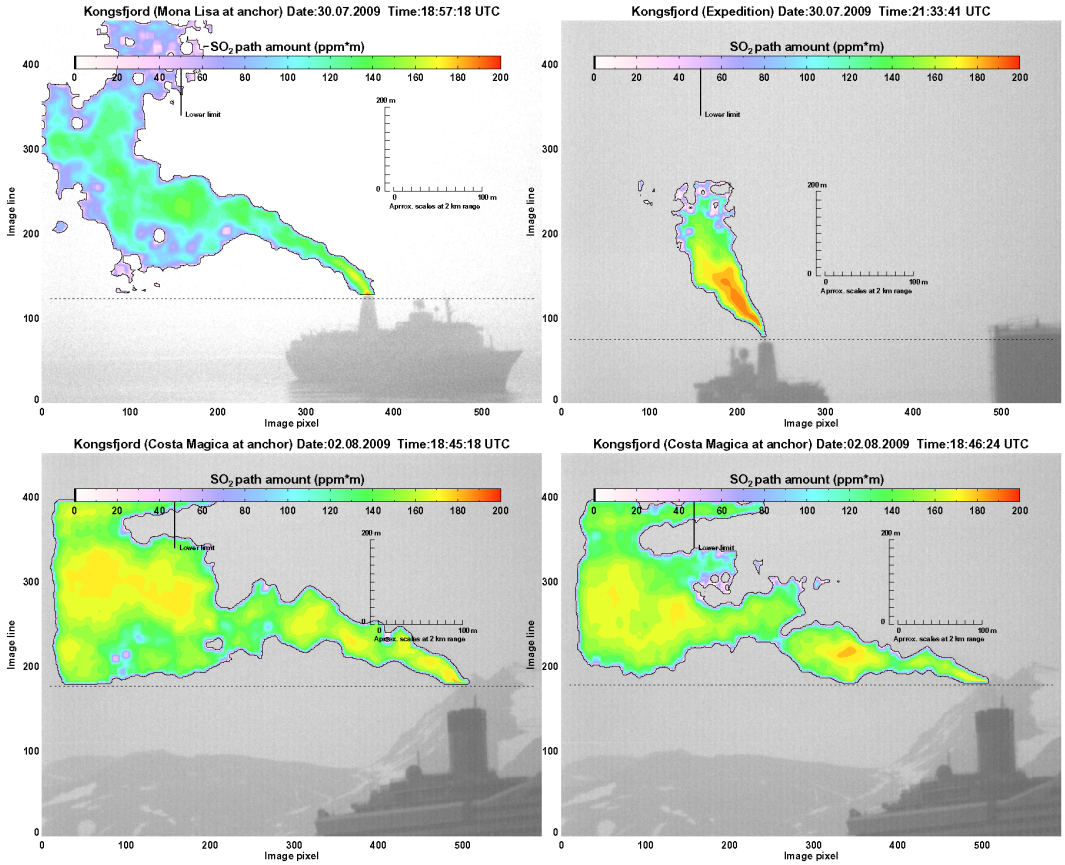

Fig. 3. SO_2 path amounts retrieved from the UV camera for three different vessels in Konsfjord at anchor or slowly manoeuvering.

AMTD
6, 9467–9511, 2013

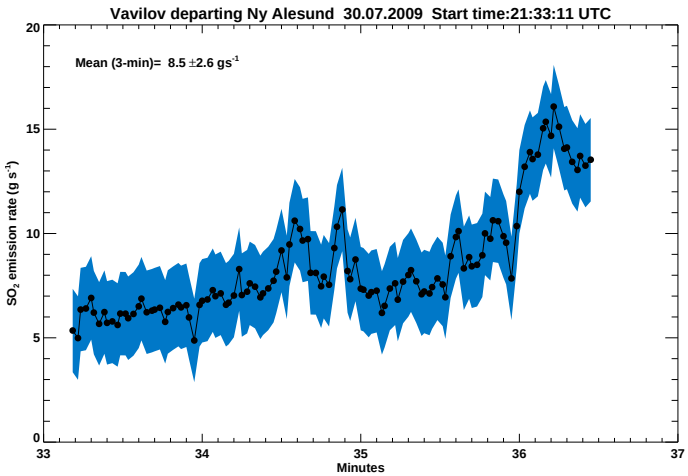

Fig. 4. SO_2 emission rate for the *SS Vavilov*. The shaded region (in blue) represents the standard deviation of measurements averaged over ~ 1 s.

AMTD
6, 9467–9511, 2013

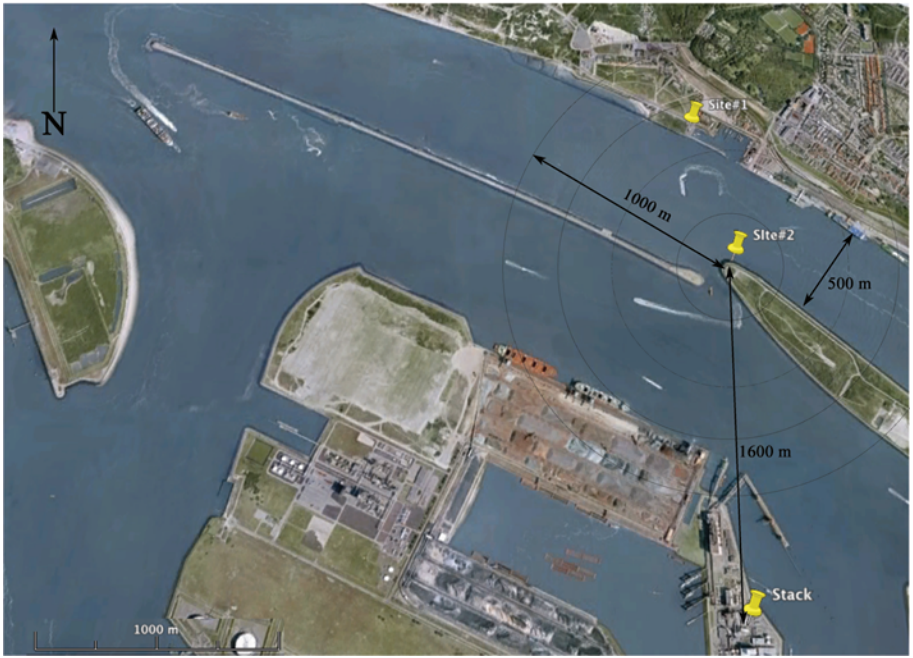

Fig. 5. Map of the shipping lanes at Hoek van Holland. The measurement sites are marked (site #1 and site #2) and the location of a nearby stack, used to verify the distance measurements is also indicated. Ships moving along the shipping lane (inbound and outbound – to the WNW) were measured at distances varying from 100 to 2000 m. The scale shown is approximate.

AMTD
6, 9467–9511, 2013

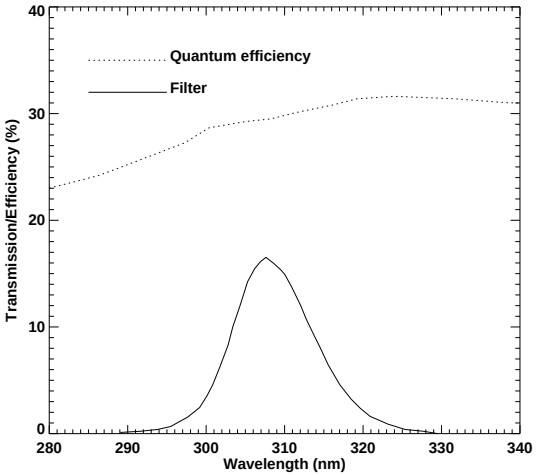

Fig. 6. The Melles-Grioot 310PB10 UV narrowband filter transmission and the Hamamatsu CCD quantum efficiency as a function of wavelength.

AMTD
6, 9467–9511, 2013

Fig. 7. Photograph of the UV camera mounted on a tripod with laptop and camera box.

AMTD
6, 9467–9511, 2013

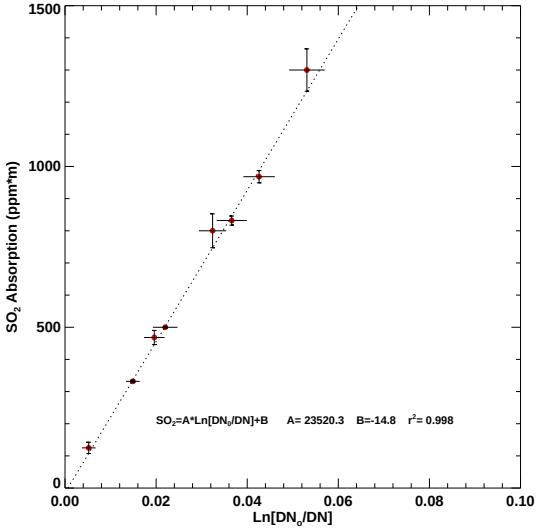

Fig. 8. Calibration curve determined used bright diffuse skylight as a source and SO_2 path amounts (in ppm m) in quartz glass cells. The SO_2 cell path amounts were independently measured using a spectrometer.

AMTD
6, 9467–9511, 2013

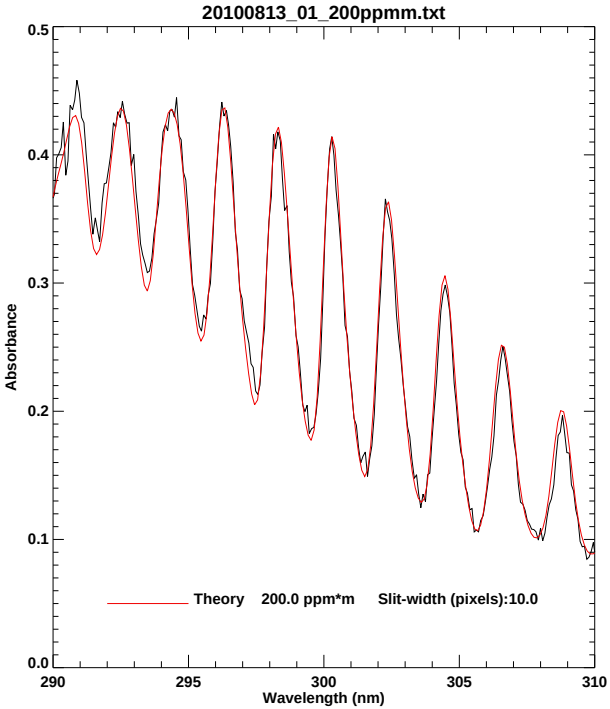

Fig. 9. Spectrometer measurements of the absorbance of UV light through a quartz cell containing SO_2 gas. The red line shows the theoretical variation of the absorbance with wavelength, based on the absorption coefficient data of Vandalae et al. (1994).

AMTD
6, 9467–9511, 2013

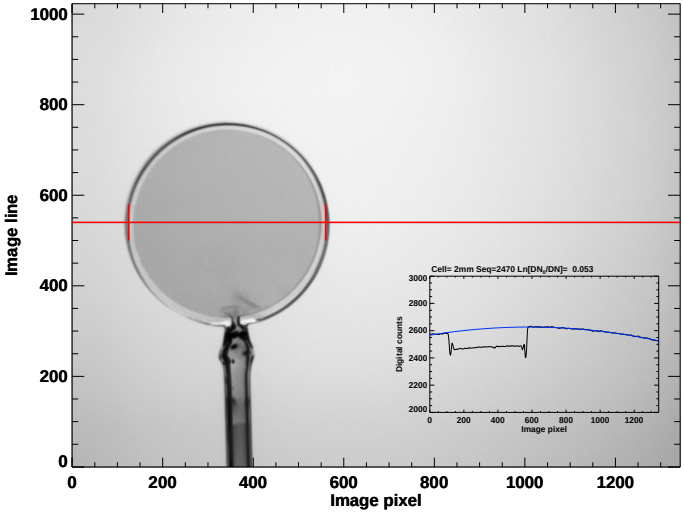

Fig. 10. Camera calibration using a bespoke SO_2 cell. The inset plot shows the intensity variation along the red line that cuts through a central part of the cell. The image counts (digital counts or digital numbers) is reduced as the light is attenuated by the SO_2 in the cell. The blue line is the Gaussian-cubic fit to the counts. The rapid variations near at the start and end of the intensity drop are due to the edges of the quartz cell and are removed before processing.

AMTD
6, 9467–9511, 2013

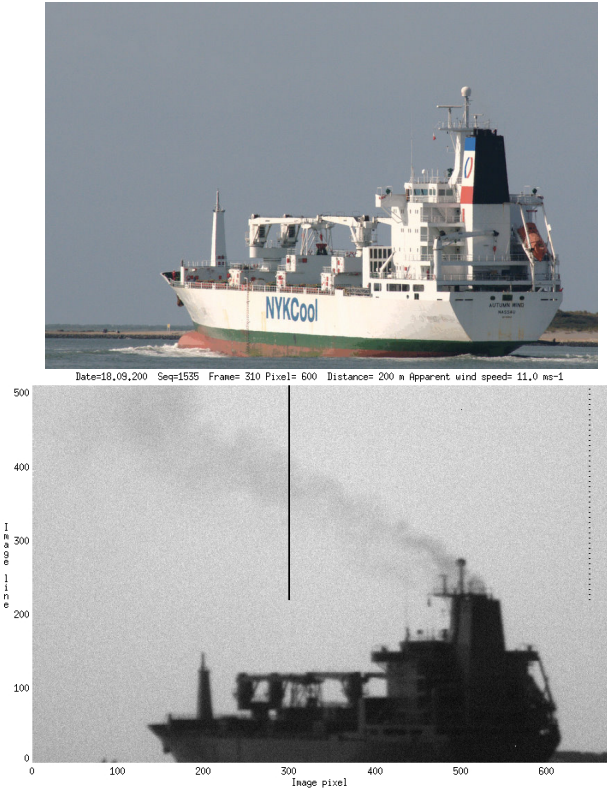

Fig. 11. Top panel: visible image of the *NYK Cool* (IMO 9038323). Bottom panel: UV image of the same ship. The black line shows the location of the vertical transect through the plume; the dashed line shows the location of the reference vertical profile.

AMTD
6, 9467–9511, 2013

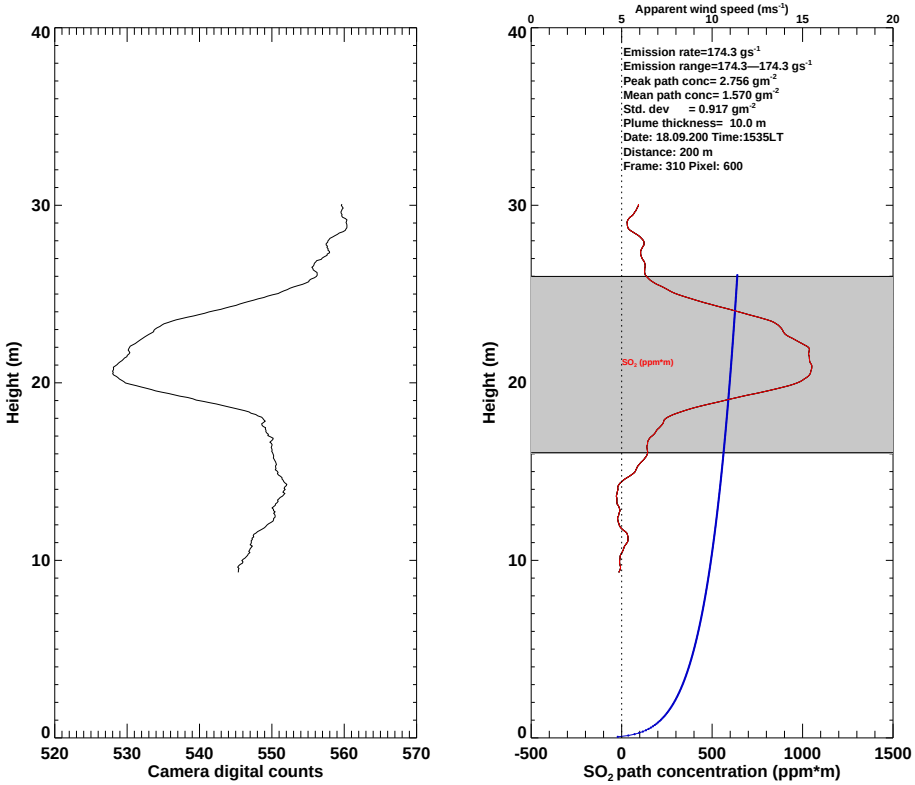

Fig. 12. SO_2 path concentration (u, in ppm m for *NYK Cool*.

AMTD
6, 9467–9511, 2013

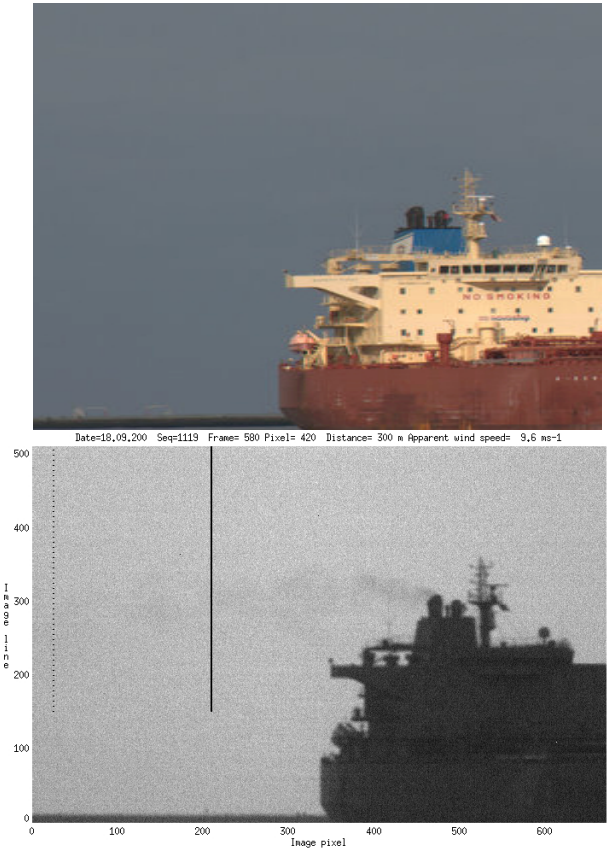

Fig. 13. Top panel: visible image of *NS Concept* (IMO 9299692) under steam into Hoek van Holland. Bottom panel: UV image of the same ship. The black line shows the location of the vertical transect through the plume; the dashed line shows the location of the reference vertical profile.

AMTD
6, 9467–9511, 2013

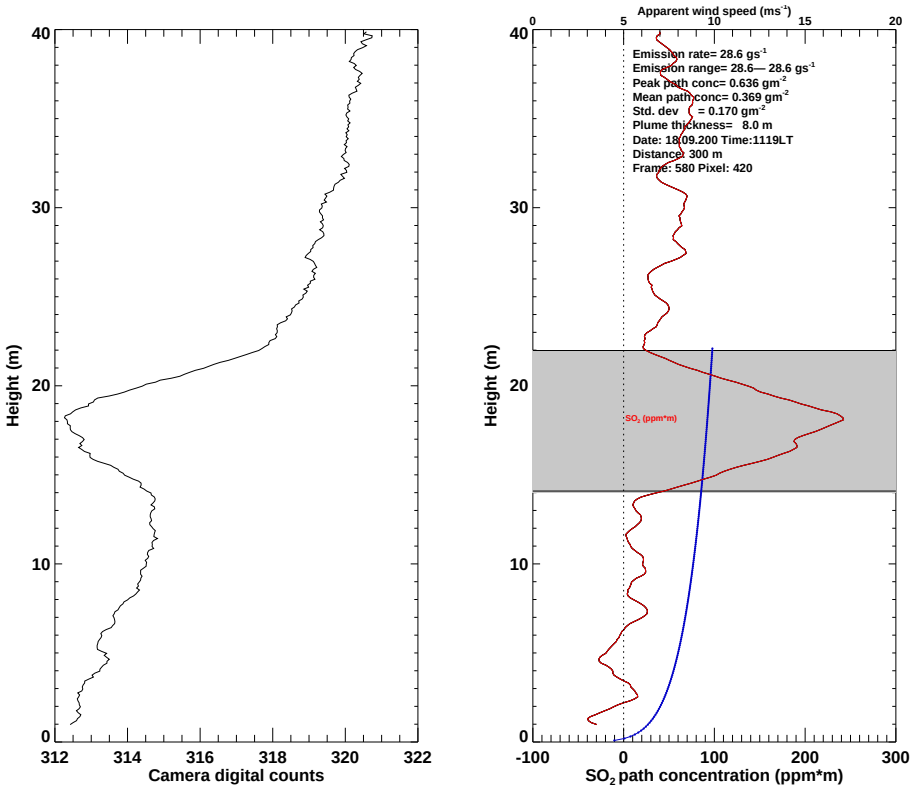

Fig. 14. SO_2 path concentration (u, in ppm m for the *NS Concept*.

AMTD
6, 9467–9511, 2013

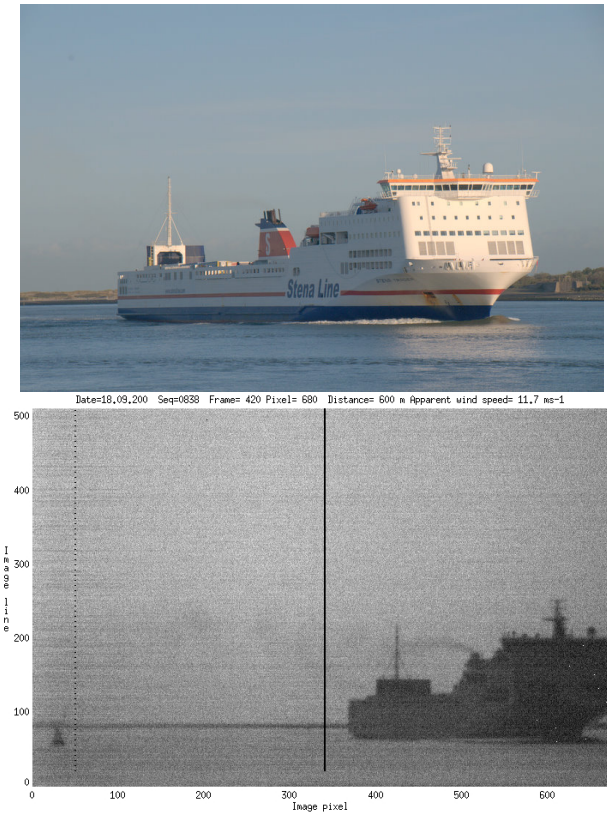

Fig. 15. *Stena Hollandica* under steam. Top panel: visible photograph. Bottom panel: UV image of SO_2 path concentration (u, in gm^{-2} or ppm m. The black line shows the location of the vertical transect through the plume; the dashed line shows the location of the reference vertical profile.

AMTD
6, 9467–9511, 2013

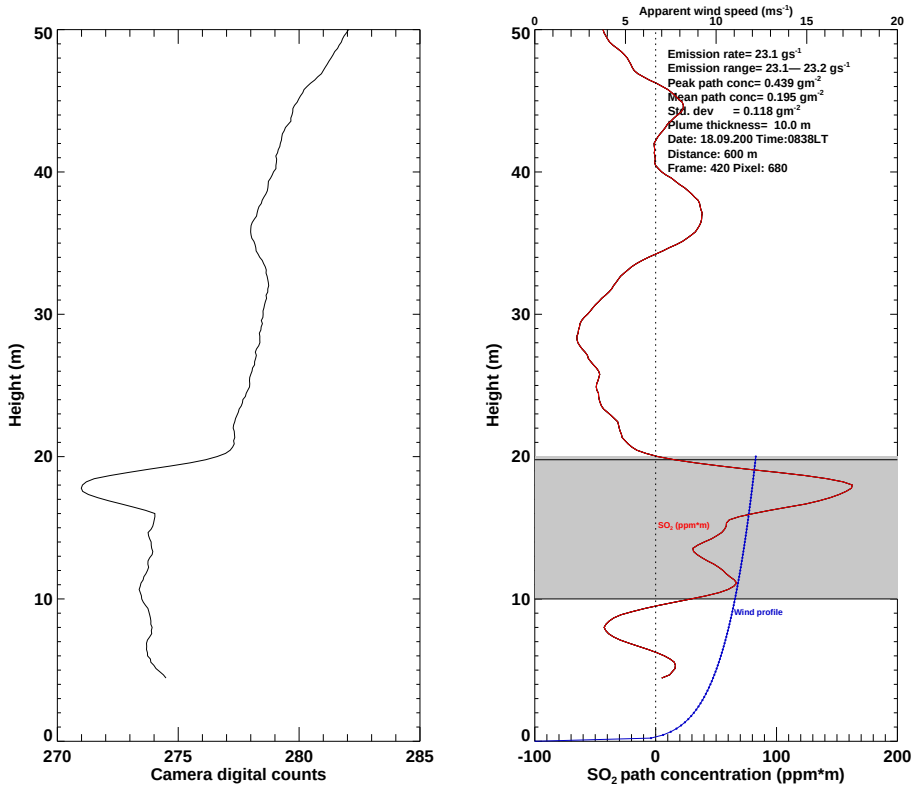

Fig. 16. SO_2 path concentration (*u*, in ppm m for the *Stena Hollandica*.

AMTD
6, 9467–9511, 2013

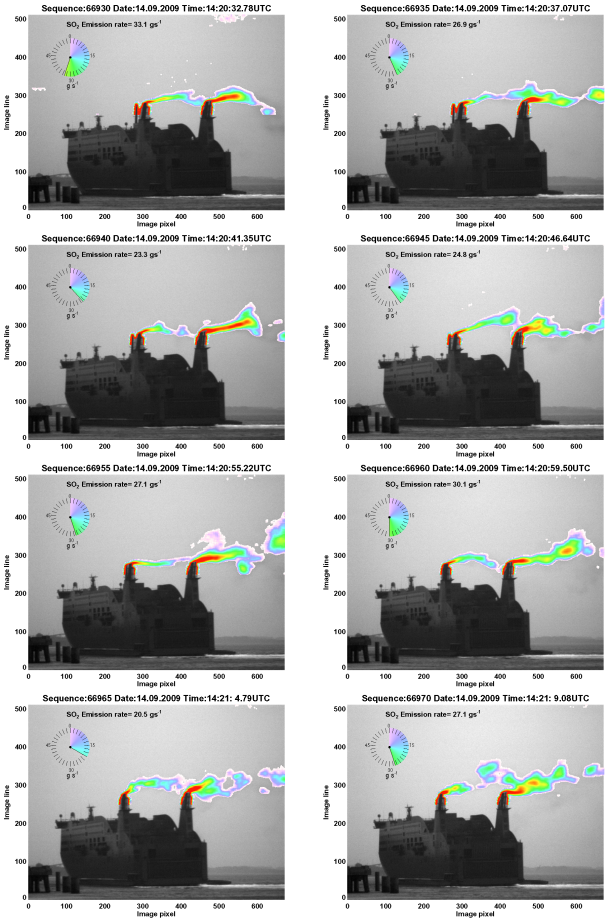

Fig. 17. Emission rate estimates from the UV camera or the *Stena Hollandica* manoeuvring at dock on 14 September 2009. Images are between 5–10 s apart from a sequence acquired at 1 s intervals.

AMTD
6, 9467–9511, 2013